

(CW)和逆时针(CCW)方向上调制光的相位。

宽谱光源 ASE 发出的光通过环形器的端口 1 进入,环形器端口 2 的输出光进入 MIOC 后等比分成顺逆两束光并通过耦合器进入谐振腔,发生陀螺效应的两路光回到 MIOC 合光干涉,并输入到环形器的端口 2,从端口 3 输入到光电探测器(PD)后转换为电信号。MIOC 的调制两臂分别输入调制信号和反馈信号,调制信号用于调制解调,反馈端用于闭环控制。

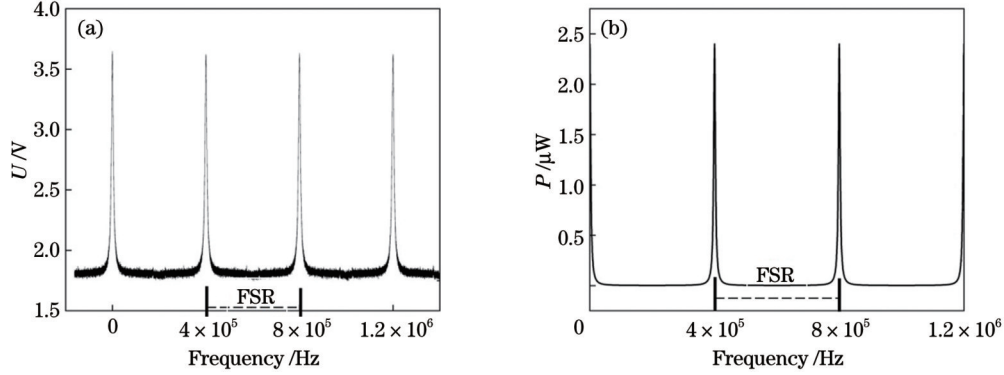


图 2 宽谱光源驱动 RFOG 的谐振曲线。(a) 仿真结果;(b) 扫模曲线

Fig. 2 Resonance curves of broadband source-driven RFOG. (a) Simulation result; (b) sweep curve

常用宽谱光源的光谱通常呈高斯分布,可以用高斯函数表示:

$$S_E(\nu) = \frac{I_0}{B} \sqrt{\frac{4 \ln 2}{\pi}} \exp \left[-4 \ln 2 \frac{(\nu - \nu_0)^2}{B^2} \right], \quad (1)$$

式中: I_0 为光源强度; ν_0 为中心频率; B 为光谱谱宽。

RIN 是指光源输出能量的振荡,这是由宽谱光源的各种傅里叶分量之间的拍频引起的附加噪声,反映了光源的振幅特性,因此 RIN 可以表示为频谱自相关的归一化,即

$$\eta_{\text{RIN}} = \frac{S_E(\nu) \star S_E(\nu)}{P_0^2}, \quad (2)$$

式中: \star 表示单侧自相关; $P_0 = \int_0^\infty S_E(\nu) d\nu$ 为光谱的积分,即平均光功率。

图 3 所示为 ASE 的光谱和 RIN 频谱。在检测带

宽谱光源驱动 RFOG 谐振曲线的仿真结果和扫模曲线如图 2 所示,仿真和实测的自由光谱范围(FSR)均为 400 kHz,实测扫模曲线受到探测背景噪声的影响,最小值不为 0。宽带光源的低相干性削弱了陀螺系统中寄生噪声的影响,提高了检测噪声的占比。抑制来自光源的噪声是提高陀螺仪精度的必要手段。检测噪声的主要类型包括热噪声、散粒噪声和强度噪声。

宽内,RIN 可视为白噪声,式(2)可简化为

$$S_{\text{RIN}} = \frac{1}{B}. \quad (3)$$

散粒噪声是光子转化为电子时产生的随机噪声,是光纤陀螺中最基本的噪声源,构成了 RFOG 的基本测量极限。散粒噪声由光子噪声和暗电流组成,与光电流线性相关。热噪声是指探测器中跨阻放大器反馈电阻的 Johnson 噪声,主要与温度有关,与光电流无关。因此,检测噪声可表示为

$$S_{\text{total}} = S_{\text{shot}} + S_{\text{thermal}} + S_{\text{RIN}} = 2e\eta I_0 + \frac{4KT}{R} + \frac{\eta^2 I_0^2}{B}, \quad (4)$$

式中: S 为噪声功率谱,其下标对应于 3 种类型的噪声; e 为电荷; η 为探测器的量子效率; I_0 为检测器的平均电流; T 为以开尔文为单位的绝对温度; K 为玻尔兹曼常数; R 为有效负载电阻。

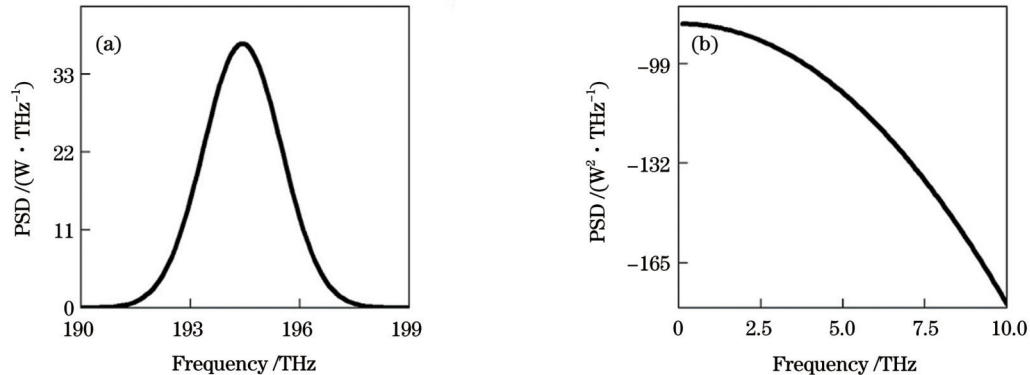


图 3 光源光谱仿真。(a) 宽带光源的光谱;(b) 宽带光源的 RIN 光谱

Fig. 3 Simulation of light source spectra. (a) Optical spectrum of broadband source; (b) RIN spectrum of broadband source

图 4 显示了检测噪声光电流的平方与 ASE 的输出光功率之间的关系。当 ASE 的输出功率超过 3 mW 时,检测噪声由 RIN 主导,热噪声和散粒噪声的影响不显著。随着光功率的增加,RIN 成为随机游走误差的主要来源。

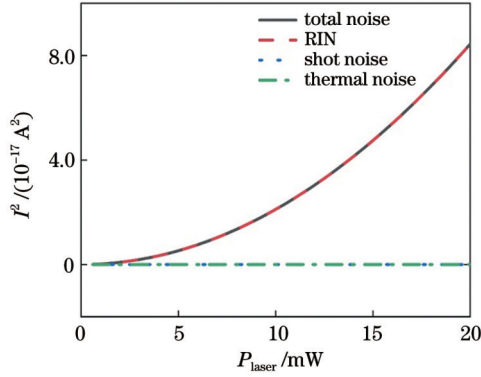


图 4 检测噪声的光电流

Fig. 4 Detected noise photocurrent

3 谐振腔中的 RIN

以上分析讨论了 ASE 光源中 3 种类型的探测噪声。接下来,将结合光纤环形谐振腔的影响,研究在基于 ASE 驱动的光纤陀螺仪中谐振腔 RIN 的理论模型。光纤环形谐振腔的谐振特性将改变 RIN 的频谱。光

纤环形谐振腔的传递函数可以表示为

$$H(\nu) = \frac{(1 - \alpha_c)k}{1 - (1 - \alpha_c)(1 - k)(1 - \alpha_L) \exp\left(j \frac{2\pi\nu}{\Delta\nu_{\text{FSR}}}\right)}, \quad (5)$$

式中: k 为光纤耦合器的分光比; ν 为光学频率; α_c 为耦合器损耗; α_L 为光纤损耗; $\Delta\nu_{\text{FSR}}$ 为谐振腔的 FSR。

穿过光纤环形谐振腔后,ASE 的光谱特性发生变化,RIN 的表达式也会发生变化,即

$$\eta_{\text{RIN,FR}} = \frac{1}{B} H_{\text{FR}}(\nu) = \frac{1}{B} \frac{|H(\nu)|^2 \star |H(\nu)|^2}{\int_0^\infty |H(\nu)|^2 d\nu}, \quad (6)$$

式中: $H_{\text{FR}}(\nu)$ 为 RIN 在谐振腔中的传递函数。

ARW 可表示陀螺中噪声的大小:

$$\zeta_{\text{ARW}} = \frac{1}{K_s \sqrt{2e\eta I_0 + \frac{4KT}{R} + \frac{\eta^2 I_0^2}{B} H_{\text{FR}}(\nu)}} = \frac{1}{K_s \sqrt{\frac{2e}{\eta I_0} + \frac{4KT}{R} \frac{1}{\eta^2 I_0^2} + \frac{1}{B} H_{\text{FR}}(\nu)}}, \quad (7)$$

式中:比例因子为 $K_s = \frac{d}{n_0 \lambda}$; n_0 为光纤的折射率; d 为光纤环的直径; λ 为波长。

图 5(a)显示了光纤环形谐振腔的传递函数,它定义了谐振腔的光谱特性。因此,当光通过谐振腔时,

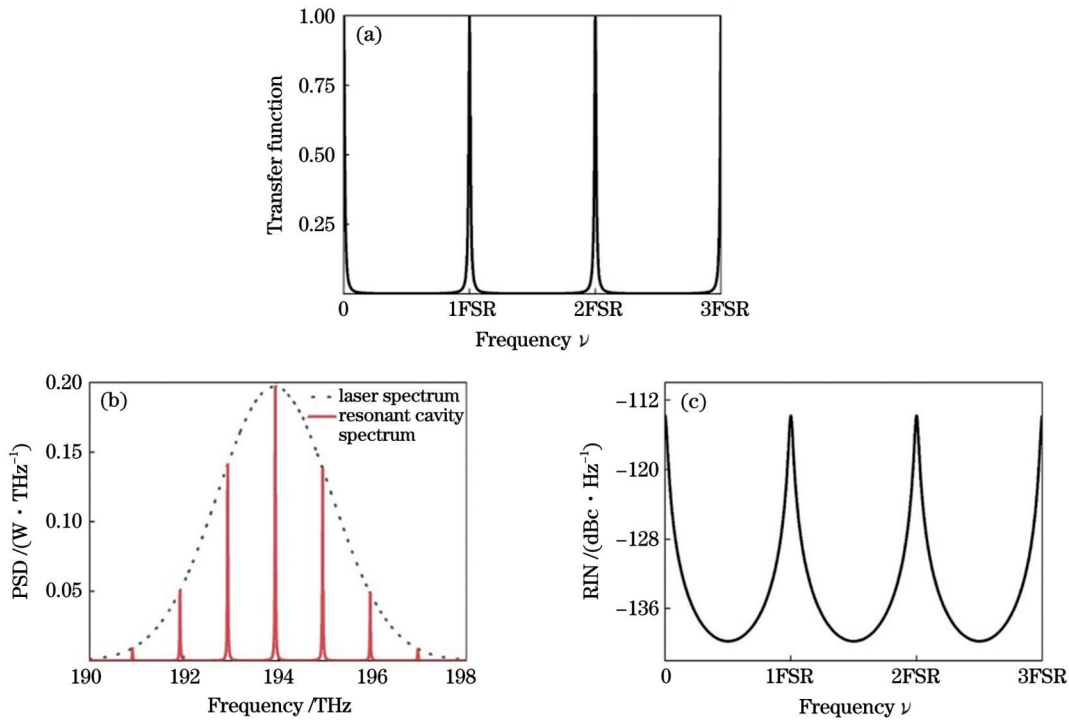


图 5 谐振腔中 RIN 的产生过程。(a) 光纤环形谐振腔的传递函数;(b) 通过光纤环形谐振腔前后的光谱(黑色虚线:光源的光谱;红色实线:通过光纤环形谐振腔后的光谱);(c) 光纤环形谐振腔的 RIN 光谱

Fig. 5 Generation process of RIN in the fiber ring resonator. (a) Transfer function of the fiber ring resonator; (b) spectra before and after passing through fiber ring resonator (black dashed line: spectrum of the source; red solid line: spectrum after passing through fiber ring resonator); (c) RIN spectrum of fiber ring resonator

光谱被整形。图 5(b) 显示了谐振腔滤波前后的光谱, 表明光源光谱影响光纤环形谐振腔的输出光谱, 并且光纤环谐振腔的 RIN 将受到光源的 RIN 的限制。图 5(c) 所示为光纤环形谐振腔的 RIN 光谱, 其周期与谐振腔的传递函数周期相同。在半个周期内, 高频 RIN 较小, 因此高频调制可以有效地抑制 RFOG 中的 RIN。

图 6 所示为到达探测器的光功率与 3 种噪声 ARW 的关系。当光功率小于 $1 \mu\text{W}$ 时, 散粒噪声比 RIN 大 2 倍, 散粒噪声的数量级与总噪声相当; 当光功率超过 $3 \mu\text{W}$ 时, RIN 比散粒噪声大 5 倍, RIN 对 ARW 的影响最为显著, 成为 3 种类型噪声中的主导因素; 热噪声占比较小。因此, 研究 RIN 并抑制 RIN 是目前提高陀螺仪性能的首要任务。

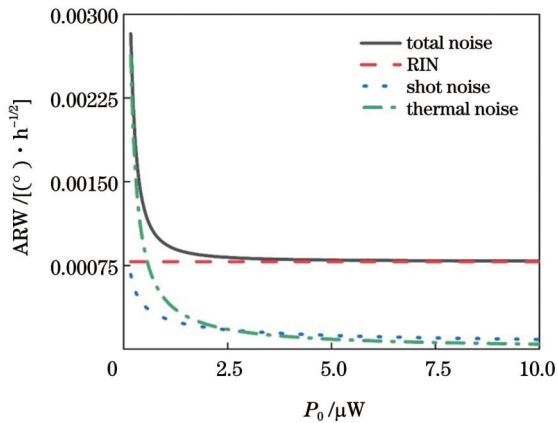


图 6 到达探测器的光功率与角度随机游走之间的关系
Fig. 6 Relationship between light power reaching the detector and angle random walk

4 实验

为了验证宽谱光源驱动 RFOG 中 RIN 模型的正确性, 测试了不同耦合器分光比的光纤环形谐振腔的 RIN。宽谱光源驱动 RFOG 系统如图 7 所示。光路系统包括宽谱光源、环形器、MIOC、谐振腔; 探测系统包括 PD、FPGA、转台。

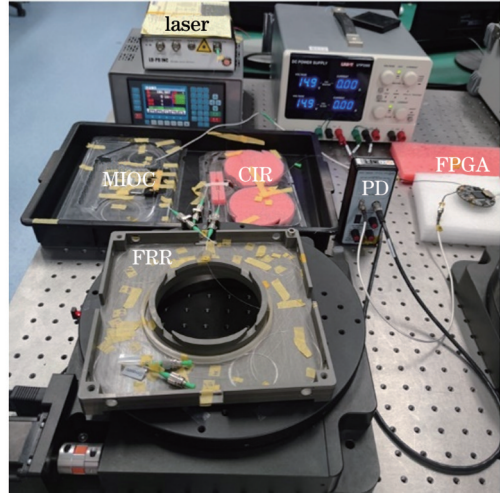


图 7 宽谱光源驱动 RFOG 系统
Fig. 7 Photograph of RFOG system

实验谐振腔参数如下: 3 个谐振腔的长度均为 500 m , 分光比分别为 $98:2$ 、 $97:3$ 、 $95:5$ 。ASE 的中心波长为 1542 nm , 谱宽为 55 nm , 输出功率为 100 mW 。

如图 8 所示, 理论与实际情况一致, RIN 的周期为 FSR。当耦合器分光比为 $98:2$ 时, 精度最高, 峰谷最低。当使用高频调制时, RIN 的影响最小。

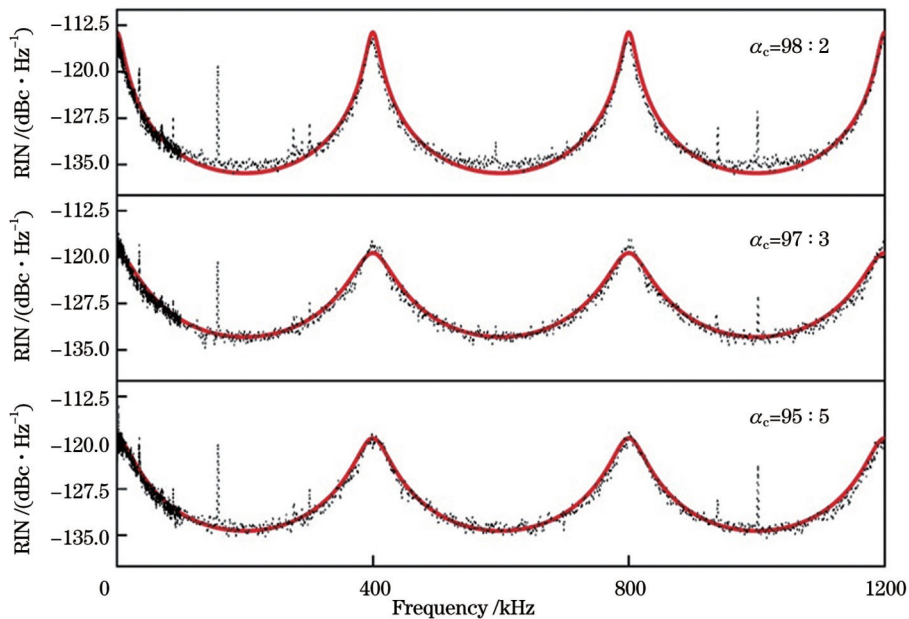


图 8 不同分光比谐振腔的 RIN 测量和理论值对比 (红色实线: 理论曲线; 黑色圆点曲线: 测量曲线)
Fig. 8 RIN measurement and theoretical values of different spectral ratio resonators (red solid line: theoretical curve; black polka dot: measurement curve)

图 9 展示了激光器谱宽分别为 50 nm 和 55 nm 时陀螺的 Allan 方差。当激光器谱宽为 50 nm 时,陀螺的角度随机游走为 $0.00437 (^{\circ})/h^{1/2}$;当激光器谱宽为 55 nm 时,陀螺的角度随机游走为 $0.00379 (^{\circ})/h^{1/2}$ 。可以看出,提高光源的谱宽,光源的 RIN 随之降低,陀螺系统的噪声也会减小,角度随机游走值提升了 13.3%。

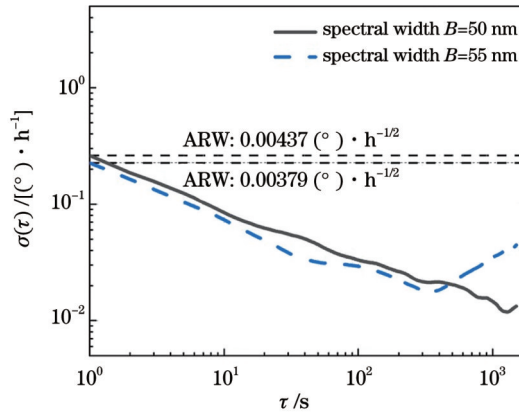


图 9 不同激光器谱宽的陀螺 Allan 方差

Fig. 9 Allan variance of gyroscope for different laser bandwidths

上述两组实验说明 RFOG 的 RIN 同时受光源谱宽和谐振腔参数的影响,验证了 RFOG 中 RIN 理论模型的正确性。

5 结 论

宽带光源提高了陀螺仪的精度,但系统中的 RIN 仍然阻碍了 RFOG 达到理论精度。因此,在前人研究的基础上,本文研究了谐振腔分光比和光源谱宽对谐振腔中 RIN 的影响,建立了谐振腔 RIN 的理论模型,并分别测试了分光比为 98:2、97:3、95:5 的 500 m 谐振腔的 RIN 和激光器谱宽为 50 nm、55 nm 时的 Allan 方差曲线。实验结果表明,增大激光器谱宽和提高谐振腔精度,均会减小 RIN 对陀螺精度的影响。这为抑制宽谱光源驱动 RFOG 的 RIN 从而提升陀螺精度提供了理论依据。当前宽谱光源驱动 RFOG 的最佳角度随机游走约为 $0.002 (^{\circ}) \cdot h^{-1/2}$,RIN 的降低将进一步提升陀螺精度,宽谱光源驱动 RFOG 具有高精度、小体积、低功耗的特点,具有良好的应用前景。

参 考 文 献

- [1] 雷明,李豪伟,于晓之,等.集成化光纤陀螺发展现状及趋势[J].半导体光电,2022,43(4):666-671.
Lei M, Li H W, Yu X Z, et al. Development status and trend of integrated fiber optic gyroscope[J]. Semiconductor Optoelectronics, 2022, 43(4): 666-671.
- [2] Strandjord L K, Qiu T, Salit M, et al. Improved bias performance in resonator fiber optic gyros using a novel modulation method for error suppression[C]//26th International Conference on Optical Fiber Sensors, September 24-28, 2018,

Lausanne. Washington, DC: OSA, 2018: ThD3.

- [3] Sanders G A, Strandjord L K, Williams W, et al. Improvements to signal processing and component miniaturization of compact resonator fiber optic gyroscopes[C]//2018 DGON Inertial Sensors and Systems (ISS), September 11-12, 2018, Braunschweig, Germany. New York: IEEE Press, 2018.
- [4] Sakr H, Chen Y, Jasion G T, et al. Hollow core optical fibres with comparable attenuation to silica fibres between 600 and 1100 nm[J]. Nature Communications, 2020, 11: 6030.
- [5] Sanders G A, Taranta A A, Narayanan C, et al. Hollow-core resonator fiber optic gyroscope using nodeless anti-resonant fiber [J]. Optics Letters, 2021, 46(1): 46-49.
- [6] Wang Z, Wang G C, Gao W, et al. Suppression of Kerr-effect induced error in resonant fiber optic gyro by a resonator with spun fiber[J]. Optics Express, 2021, 29(13): 19631-19642.
- [7] 李汉钊,钱伟文,刘路,等.谐振式光纤陀螺角度随机游走的分析与优化[J].中国激光,2021,48(9):0901002.
Li H Z, Qian W W, Liu L, et al. Analysis and optimization of angle random walk of resonant fiber optic gyroscope[J]. Chinese Journal of Lasers, 2021, 48(9): 0901002.
- [8] 马家君,刘清杨,吕嫣然,等.基于FPGA的光纤陀螺RLS自适应实时降噪技术[J].中国激光,2022,49(21):2106004.
Ma J J, Liu Q Y, Lü Y R, et al. RLS adaptive real-time noise reduction technology for fiber optic gyroscope based on FPGA [J]. Chinese Journal of Lasers, 2022, 49(21): 2106004.
- [9] 顾帅,皮鹏程,廉正刚,等.面向光纤陀螺发展需求的空芯微结构光纤的弯曲特性研究[J].中国激光,2023,50(6):0606003.
Gu S, Pi P C, Lian Z G, et al. Research on bending characteristics of hollow-core micro-structured fibers for development of fiber optic gyroscopes[J]. Chinese Journal of Lasers, 2023, 50(6): 0606003.
- [10] Zhao S X, Liu Q W, Liu Y Y, et al. Navigation-grade resonant fiber-optic gyroscope using ultra-simple white-light multibeam interferometry[J]. Photonics Research, 2022, 10(2): 542.
- [11] Morkel P R, Laming R I, Payne D N. Noise characteristics of high-power doped-fibre superluminescent sources[J]. Electronics Letters, 1990, 26(2): 96-98.
- [12] 刘霜,李汉钊,刘路,等.激光器频率噪声功率谱密度测试技术及在谐振式光纤陀螺中的应用[J].光学学报,2021,41(13):1306010.
Liu S, Li H Z, Liu L, et al. Laser frequency noise power spectral density measurement technology and its application to resonant optical fiber gyroscope[J]. Acta Optica Sinica, 2021, 41(13): 1306010.
- [13] Zheng Y, Zhang C X, Li L J. Influences of optical-spectrum errors on excess relative intensity noise in a fiber-optic gyroscope [J]. Optics Communications, 2018, 410: 504-513.
- [14] Liu S, Liu L, Hu J Y, et al. Reduction of relative intensity noise in a broadband source-driven RFOG using a high-frequency modulation technique[J]. Optics Letters, 2022, 47(19): 5100-5103.
- [15] Lefèvre H C. Potpourri of comments about the fiber optic gyro for its 40th anniversary, and how fascinating it was and it still is![J]. Proceedings of SPIE, 2016, 9852: 985203.
- [16] Shin S, Sharma U, Tu H H, et al. Characterization and analysis of relative intensity noise in broadband optical sources for optical coherence tomography[J]. IEEE Photonics Technology Letters, 2010, 22(14): 1057-1059.
- [17] Ying K, Chen D J, Pan Z Q, et al. All-optical noise reduction of fiber laser via intracavity SOA structure[J]. Applied Optics, 2016, 55(29): 8185-8188.
- [18] 胡旭东,吉世涛,洪伟,等.高精度光纤陀螺相对强度噪声抑制技术[J].科学技术创新,2022(1):25-28.
Hu X D, Ji S T, Hong W, et al. Relative intensity noise reduction technology of high precision fiber optic gyroscope[J]. Scientific and Technological Innovation, 2022(1): 25-28.

- [19] Guattari F, Moluçon C, Bigueur A, et al. Touching the limit of FOG angular random walk: challenges and applications[C]//2016 DGON Inertial Sensors and Systems (ISS), September 20–21, 2016, Karlsruhe, Germany. New York: IEEE Press, 2016.
- [20] Guattari F, Chouvin S, Moluçon C, et al. A simple optical technique to compensate for excess RIN in a fiber-optic gyroscope[C]//2014 DGON Inertial Sensors and Systems (ISS), September 16–17, 2015, Karlsruhe, Germany. New York: IEEE Press, 2014.

Principle of Relative Intensity Noise in Broadband Source-Driven Resonant Fiber Optic Gyroscope

Cheng Jun¹, Cao Kangyuan², Wu Fan², Lan Shiqi², Ye Changjiang¹, Liu Yuanyi¹, Li Jun^{2**}, Qi Xinyuan^{1*}

¹*School of Physics, Northwest University, Xi'an 710127, Shaanxi, China;*

²*Aircraft Control Integration Technology Key Laboratory of Defense Science and Technology, Flight Automatic Control Research Institute, Xi'an 710076, Shaanxi, China*

Abstract

Objective The resonant fiber optic gyroscope (RFOG) represents a cutting-edge generation of fiber optic inertial devices, leveraging the Sagnac effect within a fiber optic ring resonator. It gauges the angular velocity of external rotation by measuring the resonant frequency difference of light beams traveling clockwise and counterclockwise in the fiber optic ring resonator. In comparison to interferometric fiber optic gyroscopes, the RFOG offers advantages such as reduced length, compact dimensions, minimal thermal nonreciprocal noise, heightened detection accuracy, a wide dynamic range, and superior theoretical accuracy. Nevertheless, the progress of RFOGs is constrained by noise factors such as polarization fluctuations, the optical Kerr effect, and Rayleigh backscattering within the resonator. To address these limitations, the broadband source-driven RFOG emerges by mitigating parasitic noise through its low coherence. However, the current challenge lies in detection noise, particularly relative intensity noise (RIN), serving as the primary impediment to accuracy. Consequently, there is a pressing need to formulate a comprehensive theoretical model for RIN in broadband source-driven RFOGs. Such a model serves as the foundational framework for devising various schemes aimed at suppressing RIN, thereby advancing the precision of these gyroscopes. We fulfill this need by establishing a theoretical model grounded in the spectral width of the broadband source and resonator parameters.

Methods Regarding our need to construct a theoretical model for RIN in a broadband light source-driven RFOG, we choose an amplified spontaneous emission (ASE) with a center wavelength of 1550 nm as light source (Fig. 1 and Fig. 2). The power spectral density of the system is comprehensively analyzed to delineate the spectral alterations induced by the resonant cavity's characteristics in response to RIN (Fig. 5). To ascertain the primary contribution of the existing RIN, we employ the random walk method, which is visually depicted in Fig. 6. The validity of our theoretical model is subsequently corroborated through practical measurements involving the RIN spectrum across varying spectral ratios of the resonant cavity, and the Allan variance is assessed for diverse laser spectral widths (Fig. 8 and Fig. 9). These experimental validations solidify the reliability and applicability of our proposed theoretical framework.

Results and Discussions In the broadband source-driven RFOG, an ASE with a center wavelength of 1550 nm serves as the light source. The sensing device is a 500 m fiber ring resonator with a diameter of 12 cm. Experimental measurements of the RIN spectrum for the resonator with different splitting ratios and the Allan variance for varying laser spectral widths are presented in Fig. 8 and Fig. 9. Notably, the observed RIN spectrum aligns closely with the theoretical predictions, validating the accuracy of our proposed model. Crucially, our results demonstrate that increasing the laser spectral width is beneficial for enhancing the angle random walk performance of the gyroscope. This observation underscores the practical significance of our theoretical framework and suggests a promising avenue for optimizing gyroscope performance through spectral width modulation. These findings provide valuable insights into the field, emphasizing the potential for improved gyroscope precision through strategic adjustments to laser spectral

characteristics.

Conclusions We construct a theoretical model of RIN in RFOGs driven by a broadband source. The model here proposed considers the effects of laser spectral width and resonator parameters simultaneously, making it more realistic. Power spectral density analysis of the transmission process of RIN in the gyroscope system is performed, and the influence of different system parameters on the RIN in the RFOG driven by a broadband source is obtained. A large laser spectral width and a high-precision resonator with high-frequency modulation can effectively reduce the influence of RIN. The establishment of this theoretical model provides a basis for suppressing RIN in RFOGs driven by broadband sources.

Key words fiber optics; resonant fiber optic gyroscope; relative intensity noise; fiber ring resonator; spectrum; broadband source